Scripta Materialia 117 (2016) 16–19

Contents lists available at ScienceDirect

Scripta Materialia

journal homepage: www.elsevier.com/locate/scriptamat

Cluster formation at the Si/liquid interface in Sr and Na modified Al–Si alloys

Jenifer Barrirero [a,b], Jiehua Li [c], Michael Engstler [a], Naureen Ghafoor [b], Peter Schumacher [c], Magnus Odén [b], Frank Mücklich [a,*]

[a] Department of Materials Science, Campus D3.3, Saarland University, D 66123 Saarbrücken, Germany
[b] Nanostructured Materials, Department of Physics, Chemistry, and Biology (IFM), Linköping University, SE 581 83 Linköping, Sweden
[c] Montanuniversität Leoben, A 8700 Leoben, Austria

ARTICLE INFO

Article history:
Received 21 December 2015
Received in revised form 12 February 2016
Accepted 13 February 2016
Available online xxxx

Keywords:
Eutectic solidification
Atom probe tomography
Aluminium alloys
Eutectic modification
Transmission electron microscopy

ABSTRACT

Atom probe tomography was used to compare Na and Sr modified Al–Si hypoeutectic alloys. Both Na and Sr promote the formation of nanometre-sized clusters in the Si eutectic phase. Compositional analyses of the clusters show an Al:Sr ratio of 2.92 ± 0.46 and an Al:Na ratio of 1.07 ± 0.23. It is proposed that $SrAl_2Si_2$ and NaAlSi clusters are formed at the Si/liquid interface and take part in the modification process by altering the eutectic Si growth.

To meet the evolving demands of current high-performance industrial applications, ultimate tensile strength, ductility, impact and thermal-shock properties of Al–Si alloys can be effectively favoured by a morphological modification of the eutectic phase [1]. Na and Sr are known to segregate into the eutectic Si phase and effectively induce a transition from a plate- to a coralline-like structure [2–5].

Since Pacz discovered this effect in 1921 [6], large efforts have been directed towards understanding the underlying mechanisms. During the first half of the last century, Na modification was in focus [7–12]. Later, Sr emerged as an attractive alternative to Na since it is easier to control the Sr-content during the casting process. Na has high volatility and oxidizes easily, which affects the Na addition control [8]. Sr has a lower tendency to fade and can be added in the form of Al–Sr master alloys, making the addition of the alloying element easier and more precise [1].

The effects of Na and Sr on the morphological modification have often been considered indistinctively [13–15]. Both elements produce multiplication of twins and lattice defects in the Si phase, as well as the same coralline-like eutectic microstructure.

Recent investigations have revealed that Al forms segregations with Sr or Na in the Si eutectic phase [16–18]. The presence of Al in combination with the modifier was not considered in previous theories when explaining the origin of the modification [5,11]. These findings open for new interpretations on the role of Al and the mechanisms causing the change in the microstructure.

In this paper, atom probe tomography (APT) combined with transmission electron microscopy (TEM) is used to compare the structure and the Al content in Sr- and Na-rich clusters in the Si eutectic phase. It is proposed that $SrAl_2Si_2$ and NaAlSi clusters form at the Si/liquid interface and take part in the modification of the eutectic Si growth to form a coralline-like microstructure.

Al–Si hypoeutectic alloys modified with Sr and Na were manufactured by high purity Si (5 N, 99.999) and Al (5 N). An Al-5 wt.% Si alloy was modified by 160 ppm Na. Na was added using elemental Na in vacuum packed Al foils before casting. An Al-7 wt.% Si alloy was modified by 150 ppm Sr added using an Al-10 wt.% Sr master alloy.

TEM sample preparation was performed by successive mechanical grinding, polishing, and dimpling to a thickness of about 30 μm followed by Ar ion-beam milling to electron transparency using a Gatan Precision Ion Polishing System (PIPS) model 691. Additional TEM and APT samples were prepared in a dual-beam focused ion beam/scanning electron microscopy workstation (FIB/SEM) (Helios NanoLab 600™, FEI Company, USA). After lift out and thinning of the samples, a low energy milling at 2 kV was performed to minimize gallium induced damage [19].

TEM analysis was performed using a FEI Tecnai G2 microscope operated at 200 kV in micro and nanoprobe mode and an image-side aberration-corrected JEOL 2100F microscope operated at 200 kV. Laser Pulsed APT was carried out with a LEAP™ 3000X HR (CAMECA) at repetition rates of 160 kHz and 250 kHz, a specimen temperature of about

* Corresponding author.

http://dx.doi.org/10.1016/j.scriptamat.2016.02.018
1359-6462/

40 K, a pressure lower than 1.33×10^{-8} Pa, and a laser pulse energy in the range of 0.4–0.5 nJ. The evaporation rate of the specimen was 5 atoms per 1000 pulses. Datasets were reconstructed and analysed with IVAS™ 3.6.8 software (CAMECA). Al, Sr and Na contents in Si were measured after background subtraction performed with the IVAS software.

The eutectic Si structure of both alloys, modified either by the addition of Sr or Na, presents a high density of lattice defects (Fig. 1). These defects are necessary for the repeated change of Si growth direction and growth rate that give rise to the desired coralline-structure [16]. It was observed that the defects in the Si lattice are enriched by the modifier (Sr/Na) and Al by correlating TEM and APT data. TEM images in Fig. 1 show spherical-precipitates, stacking faults (SFs) and twin lamellas (TLs) which have a one-to-one correspondence to the three categories of solute clusters detected by APT: spherical, rod-like and planar (Figs. 2 and 3).

TEM images of both alloys reveal that spherical precipitates are often located at the intersection of SFs and TLs on {111}Si planes (Fig. 1 b, c and d). APT confirms the presence of spherical precipitates and shows solute enrichment of Al and modifiers (Fig. 2). This suggests that the spherical precipitates may assist the formation of SFs and TLs. Based on this, the phenomena causing the modified microstructure appear to be the same for both Sr and Na additions, i.e. an obstructed Si growth as a result of the formation of a high number of solute-enriched clusters and crystallographic defects.

Despite the structural similarities between Sr and Na modifications, it is important to point out a significant difference in the composition of the Sr- and Na-rich clusters recorded by APT. Since the clusters are located in the Si phase, their Si content could not be determined and instead the focus was put on the content of Al and modifier. The local composition of the clusters measured by APT can be influenced by ion trajectory overlaps due to local magnification effects [20]. When considering 2–5 nm sized segregations present in these alloys, this artefact may lead to a convolution of the matrix with the precipitate resulting in an overestimation of the matrix element [20–24]. Given this uncertainty, reporting relative solute ratios Al:M (M = Sr or Na) is more adequate than the absolute concentrations. Each single cluster of solutes was exported in tightly fitted regions of interest (ROIs) for separate analysis. The bulk composition inside the ROI was measured after optimization of the elemental ranges in the mass-to-charge spectrum. The number of solute atoms in the clusters was measured after background subtraction. Fig. 4 shows the Al:M ratios for each cluster. The ratios for Sr- and Na-modified alloys are distinctly different, i.e. the ratio datasets have no overlap and no outliers. In the Sr-modified alloy, the average of 14 rod-like and 5 planar segregations from 6 APT specimens yields an Al:Sr ratio of 2.92 ± 0.46. In the Na-modified alloy, the average of 9 rod-like and 2 planar segregations from 5 APT specimens results in an Al:Na ratio of 1.07 ± 0.23. The standard deviations in the Al:M ratios can be attributed to the combined effect of the limited number of solute atoms involved in such small clusters and the detection efficiency of APT (~37%). The ratios indicate that Al is needed to form these segregations and that Al interacts differently with Na and Sr.

Inferring the role of Al on the modification and understanding the Al:M ratios is not straight forward given the required extrapolation from an observed "post-mortem" microstructure to the dynamic scenario occurring at a moving solid/liquid interface in a temperature gradient during solidification.

The high density of defects has historically been explained by the impurity induced twinning (IIT) mechanism and the poisoning of the twin plane re-entrant edge (TPRE) mechanism suggesting an inhibition of

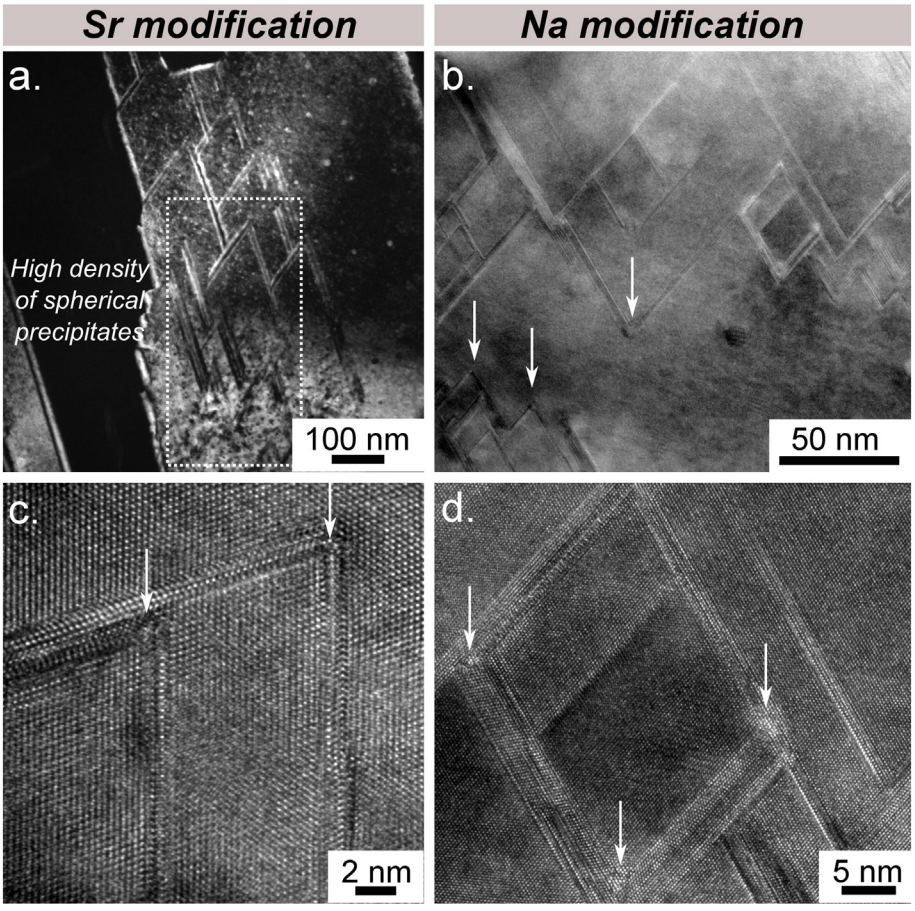

Fig. 1. TEM images of the eutectic Si phase. (a) Dark-field image of Sr-modified Si phase recorded along <111> zone axis. (b) Bright-filed image of Na-modified Si phase recorded along <011> zone axis. (c,d) High resolution images of the Sr- and Na-modified alloys, respectively. White arrows highlight particles at the intersections of SFs and TLs.

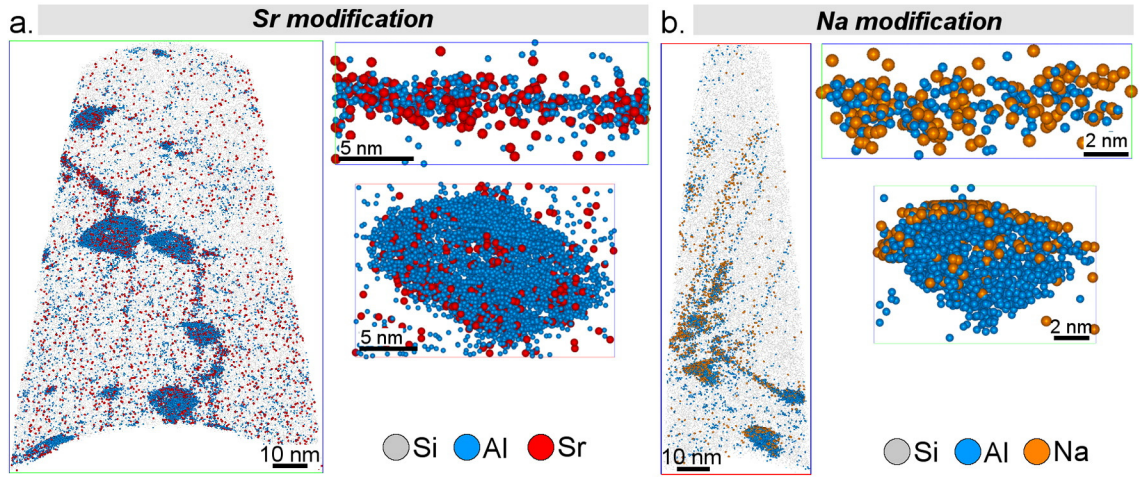

Fig. 2. APT datasets of the eutectic Si phase and magnified regions of interest of rod-like and particle-like segregations: (a) Sr-modified alloy, b) Na-modified alloy.

the Si growth by adsorption of single atoms of the modifier at the solid/liquid interface [5,11]. This led to the proposal that the atomic radius (r) of the modifiers satisfy a geometrical factor of $r_M/r_{Si} = 1.646$. However, this way of explaining the origin for modification does not consider the presence of Al nor the defined Al:M ratios found in this investigation.

Recently, Li et al. [25] proposed that the adsorption of Sr (or Na) atoms causes the changes in growth direction and multiplication of twins, while the entrainment of Al together with the modifier is an artefact rather than an active factor for the modification. They propose that the formation of Al–Si–Sr-rich clusters takes place after the adsorption of Sr (or Na) atoms during the subsequent overgrowth of Si. Another way of explaining the presence of Al, however, would be to consider the formation of such clusters at the growth front just before the overgrowth of Si. To address the different Al:M ratios, one can first consider the invariant reactions reported in literature for the Al–Si [26], Al–Si–Na [27] and Al–Si–Sr [28] systems (Table 1). Due to the low concentration of modifier in both systems, they present ternary eutectic reactions very near to the binary Al-Si eutectic composition and temperature (Table 1). In the system containing Na, the NaAlSi (τ) ternary compound forms together with Si and Al [27]; while for the alloy containing Sr, $SrAl_2Si_2$ phase is predicted [28]. Such compounds are consistent with the Al:M ratios measured by APT in the rod-like and planar segregations in the Si phase. The stoichiometry of the clusters (Al:Na ~ 1, Al:Sr ~ 2) corresponds to the compounds expected for each alloy, i.e. NaAlSi for Na modification and $SrAl_2Si_2$ for Sr modification.

In the case of the alloy containing Sr, even though thermodynamic calculations predict the formation of $SrAl_2Si_2$ at the ternary eutectic reaction [28], this will only be possible if there is a local Sr concentration of about 20 at.% Sr. Since the content of the modifier in the alloy is much lower, the nucleation and growth of this intermetallic phase will not be always feasible. However, locally at a length scale just involving a few thousand atoms the situation might be dramatically different. Ahead of the growing Si crystal a diffusion profile is formed by segregation leading to constitutional undercooling. The solubilities of Al and Sr in Si are ~400 at-ppm and ~40 at-ppm, respectively [16], which is less than the expected concentration in the liquid. Therefore, both these elements are expected to be enriched ahead of the solidification front. That is, over a distance of a few nanometres in front of the growth front, the local concentrations of Sr and Al are sufficiently high to

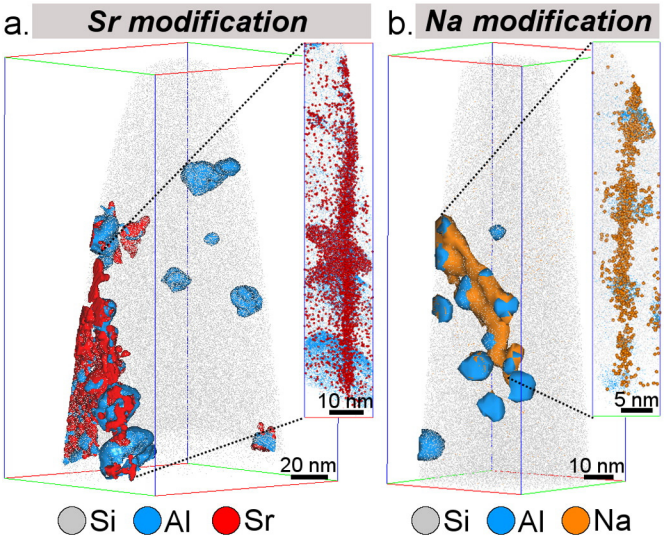

Fig. 3. APT datasets of the eutectic Si phase. Segregations are highlighted by iso-concentration surfaces. Single atoms are only shown in the insets. (a) Sr-modified alloy. Iso-concentration surfaces at 2 at.% Al and 0.4 at.% Sr, (b) Na-modified alloy. Iso-concentration surfaces at 3 at.% Al and 1 at.%Na.

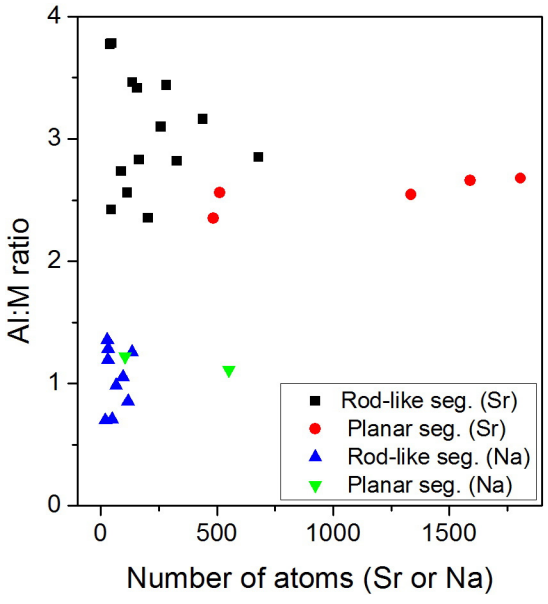

Fig. 4. Al:M (M: Sr, Na) ratios for rod-like and planar segregations.

Table 1
Eutectic reactions in the binary Al-Si and ternary Al–Si–Na and Al–Si–Sr alloys.

Reaction	T (°C)	Composition (at.%)		
(Al–Si) system [26]			Al	Si
L ↔ (Al) + (Si)	577		87.8	12.2
(Al–Si–Na) system [27]		Na	Al	Si
L ↔ AlSiNa (τ) + (Al) + (Si)	576	0.01	87.35	12.64
(Al–Si–Sr) system [28]		Sr	Al	Si
L ↔ Al_2Si_2Sr (τ_1) + (Al) + Si	575	0.03	~86.8	13.1

allow for the formation of atomic clusters of compounds. Recently, Srirangam et al. [29] showed that the local coordination environment of Sr in Al–Si alloys is consistent with the formation of $SrAl_2Si_2$ clusters in the eutectic phase supporting the concept that nanometre-sized clusters can be formed in these alloys. According to the classical homogenous nucleation theory clusters of this size are subcritical, and the local ordering in the melt would be that of fluctuating clusters. For stable clusters to occur, heterogeneous substrates and/or high undercooling must be present. Thus, during growth of the eutectic Si, two competing processes are active at the solid/liquid interface, i.e. segregation of Sr and Al out of the Si crystal and the formation of clusters where the interface acts as a heterogeneous substrate. In the case of conventional solidification, segregation dominates. However, if adsorption of a modifying element (Sr or Na) is possible, it would be energetically favourable to form clusters at the interface. These clusters are continuously incorporated into the growing Si crystal, which also seals their size and composition. The same reasoning can be used for the alloy modified by Na with the difference that the compound forming is NaAlSi. This means all of the three phases that results from the ternary eutectic reactions (Table 1) are present in the alloys, although the $SrAl_2S_{i2}$ and NaAlSi compounds cannot be resolved by optical microscope or even SEM. It remains unclear whether single modifier atoms or Al–Si–M-rich clusters induce multiplication of crystallographic defect. However, both cases highlight the interaction between the modifier and Si. Furthermore, APT shows that Al is present in all defects [16], even when the defect is only one atomic monolayer [18].

The presence of Al–Si–M-rich clusters in the eutectic phase suggests that the efficiency of a modifier depends on its ability to form ternary compound clusters at the Si/liquid interface near the binary eutectic point, and furthers the understanding of the eutectic modification of Al–Si alloys. Other elements such as Eu [30,31], Ba [32], Ca [33] and Yb [34] which are known to alter the microstructure either to fibrous Si or a refined plate-like structure can also form ternary compounds, i.e. $EuAl_2Si_2$, BaAlSi, $BaAl_2Si_2$, $CaAl_2Si_2$ and $YbAl_2Si_2$. Studies of these systems by means of APT will provide additional information towards the understanding of the eutectic modification.

In conclusion, APT chemical analysis showed that Sr and Na additions in Al–Si alloys form clusters with fixed and distinctly different Al:M ratios. Based on these results, it is proposed that $SrAl_2Si_2$ and NaAlSi clusters formed at the Si/liquid interface alter the Si growth and consequently modify the microstructure. This investigation emphasizes the importance of considering compound formation when evaluating elements for modification and optimization of manufacturing processes.

We acknowledge the fruitful discussion with Prof. Rainer Schmid-Fetzer, Dr. Songmao Liang and Hisham Aboulfadl. The present investigation is supported by the German Federal Ministry of Economics and Technology (project: AiF 17204 N), the European Regional Development Fund (AME-Lab, C/4-EFRE-13/2009/Br), the German Research Foundation (DFG) and the Federal State Government of Saarland (INST 256/298-1 FUGG). The authors thank V. Groten and Prof. Dr.-Ing. A. Bührig-Polaczek (Foundry Institute at RWTH Aachen) for providing the samples. J. Barrirero acknowledges the Erasmus Mundus Doctoral Programme DocMASE of the European Commission (FPA 2011-0020), N. Ghafoor acknowledges VINNOVA Strategic Faculty Grant VINNMER (2011-03464) Marie Curie Chair for financial support and J.H. Li acknowledges the access to TEM at the Erich Schmidt Institute of Materials Science of the Austrian Academy of Science and the financial support from the Major International (Regional) Joint Research Project (No. 51420105005) from China.

References

[1] J.E. Gruzleski, B. Closset, The Treatment of Liquid Aluminum–Silicon Alloys, American Foundrymens Society, 1990.
[2] F. Lasagni, A. Lasagni, C. Holzapfel, F. Mücklich, H.P. Degischer, Adv. Eng. Mater. 8 (2006) 719–723.
[3] L. Clapham, R.W. Smith, J. Cryst. Growth 92 (1988) 263–270.
[4] K. Nogita, H. Yasuda, K. Yoshida, K. Uesugi, A. Takeuchi, Y. Suzuki, A.K. Dahle, Scr. Mater. 55 (2006) 787–790.
[5] S. Lu, A. Hellawell, Metall. Trans. A 18 (1987) 1721–1733.
[6] A. Pacz, Alloy 1 (1921) 387,900.
[7] A.G.C. Gwyer, H.W.L. Phillips, J. Inst. Met. 36 (1923) 283–324.
[8] B.M. Thall, B. Chalmers, J. Inst. Met. 77 (1950) 79–97.
[9] R.C. Plumb, J.E. Lewis, J. Inst. Met. 86 (1958) 393–400.
[10] V.L. Davies, J.M. West, J. Inst. Met. 92 (1963) 175–180.
[11] M.G. Day, A. Hellawell, Proc. R. Soc. A Math. Phys. Eng. Sci. 305 (1968) 473–491.
[12] H. Fredriksson, M. Hillert, N. Lange, J. Inst. Met. 101 (1973) 285–299.
[13] D.C. Jenkinson, L.M. Hogan, J. Cryst. Growth 28 (1975) 171–187.
[14] M.D. Hanna, S.-Z. Lu, A. Hellawell, Metall. Trans. A 15 (1984) 459–469.
[15] K.F. Kobayashi, L.M. Hogan, J. Mater. Sci. 20 (1985) 1961–1975.
[16] J. Barrirero, M. Engstler, N. Ghafoor, N. de Jonge, M. Odén, F. Mücklich, J. Alloys Compd. 611 (2014) 410–421.
[17] M. Timpel, N. Wanderka, R. Schlesiger, T. Yamamoto, D. Isheim, G. Schmitz, S. Matsumura, J. Banhart, Ultramicroscopy 132 (2013) 216–221.
[18] J.H. Li, J. Barrirero, M. Engstler, H. Aboulfadl, F. Mücklich, P. Schumacher, Metall. Mater. Trans. A 46 (2014) 1300–1311.
[19] K. Thompson, D. Lawrence, D.J. Larson, J.D. Olson, T.F. Kelly, B. Gorman, Ultramicroscopy 107 (2007) 131–139.
[20] W. Lefebvre, F. Danoix, G. Da Costa, F. De Geuser, H. Hallem, A. Deschamps, M. Dumont, Surf. Interface Anal. 39 (2007) 206–212.
[21] G. Sha, H. Möller, W.E. Stumpf, J.H. Xia, G. Govender, S.P. Ringer, Acta Mater. 60 (2012) 692–701.
[22] B. Gault, F. de Geuser, L. Bourgeois, B.M. Gabble, S.P. Ringer, B.C. Muddle, Ultramicroscopy 111 (2011) 683–689.
[23] J. Rüsing, J.T. Sebastian, O.C. Hellman, D.N. Seidman, Microsc. Microanal. 6 (2000) 445–451.
[24] H.K. Hasting, W. Lefebvre, C. Marioara, J.C. Walmsley, S. Andersen, R. Holmestad, F. Danoix, Surf. Interface Anal. 39 (2007) 189–194.
[25] J.H. Li, M. Albu, F. Hofer, P. Schumacher, Acta Mater. 83 (2015) 187–202.
[26] J.L. Murray, A.J. McAlister, Bull. Alloy Phase Diagr. 5 (1984) 74–84.
[27] N. Bochvar, P. Budberg, F. Hayes, Y. Liberov, R. Schmid-Fetzer, Al–Na–Si Ternary Phase Diagram, MSI, Materials Science International Services GmbH, Stuttgart, 1993.
[28] R. Ferro, O. Kubaschewski, H. Hubert, G. Ibe, VCH 8 (1993) 270–278.
[29] P. Srirangam, S. Chattopadhyay, A. Bhattacharya, S. Nag, J. Kaduk, S. Shankar, R. Banerjee, T. Shibata, Acta Mater. 65 (2014) 185–193.
[30] J.H. Li, X.D. Wang, T.H. Ludwig, Y. Tsunekawa, L. Arnberg, J.Z. Jiang, P. Schumacher, Acta Mater. 84 (2015) 153–163.
[31] J. Li, F. Hage, M. Wiessner, L. Romaner, D. Scheiber, B. Sartory, Q. Ramasse, P. Schumacher, Sci. Rep. 5 (2015) 13802.
[32] A. Knuutinen, K. Nogita, S.D. Mcdonald, A.K. Dahle, 1 (2002) 229–240.
[33] T.H. Ludwig, P.L. Schaffer, L. Arnberg, Metall. Mater. Trans. A 44 (2013) 3783–3796.
[34] J.H. Li, S. Suetsugu, Y. Tsunekawa, P. Schumacher, Metall. Mater. Trans. A 44 (2012) 669–681.